SOURCE FIELD MODELING BY SELF-CONSISTENT GAUSSIAN BEAM SUPERPOSITION

L.B. Felsen, J.M. Klosner, I.T. Lu, and Z. Grossfeld

Polytechnic University
Farmingdale, NY

INTRODUCTION

Analytical modeling of ultrasound NDE requires understanding of the propagation properties of source-excited high frequency fields in an elastic environment. The sources may be actual, as generated by a transducer, or they may be induced in a fault region that disturbs the unflawed environment. One effective approach to dealing with wave phenomena in the source-excited environment is to decompose the source distribution into basis elements, propagate each basis element from the source region to the receiver, and recombine them to synthesize the total field. Because Gaussian beams have favorable propagation characteristics and represent physically observable entities, they have played a prominent role in many modeling schemes [1,2]. Gaussian beams individually may furnish an approximate replica of fields generated by ultrasonic transducers with smoothly tapered aperture distribution. These beams, because they are highly focused, are normally propagated through the environment by paraxially approximated phases and amplitudes, thereby facilitating description of beam preserving narrow-angle encounters with planar and curved interfaces, etc. [2]. However, scattering from localized fault zones or abrupt terminations is not beam preserving, and the output from many transducers (like flat pistons) gives rise to side lobes and other marked deviations from a well collimated Gaussian.

To cope with non-Gaussian effects without losing the attractiveness of the Gaussians, various efforts have been afoot to employ a distribution or superposition of Gaussian basis fields for modeling general source configurations. Some of these schemes, like those based on Hermite or Laguerre Gaussian expansions, are rigorous while others are more heuristic [1,3]. We shall introduce here a new procedure whereby an arbitrary planar source distribution is decomposed rigorously into a discrete superposition of linearly phased and nonphased Gaussian elements distributed self-consistently over a lattice in a configuration-spectral wavenumber phase space. Nonphased elements generate forward propagating beams, whereas phased elements generate tilted beams. This beam lattice synthesis has recently been applied to electromagnetic and acoustic fields [4], and it is here developed for elastic fields. Due to lack of space, we shall give a concise description here and reserve a more detailed version for a future publication. In what follows, the beam synthesis is summarized for two simple models of time-harmonic finite planar aperture source distributions in an unbounded elastic solid: linearly phased smoothly tapered, and abruptly truncated, aperture profiles. The problem is two-dimensional and involves compressional (P) and vertically polarized shear (SV) waves.

THEORY

An infinite homogeneous elastic isotropic medium characterized by Lamé constants λ, μ, and by density ρ is assumed to be excited by a y-independent, z-directed pressure or body force distribution f(x) (with suppressed harmonic time dependence $\exp(-i\omega t)$) acting on a plane surface z= 0 between $-a \leq x \leq a$. Following [5] the body force problem can be reformulated as a boundary value problem defined as

$$\sigma_{zz}(x,0^+) = \begin{cases} -0.5\, f(x) & , \text{ for } -a \leq x \leq a \\ 0 & , \text{ for } |x| > a \end{cases} \quad ; \quad u(x,0) = 0 \tag{1}$$

where σ_{zz} and u are, respectively, the vertical normal stress and horizontal displacement. The resulting elastic fields at $z \geq 0^+$ can be derived from two potentials $\Phi(x,z)$ and $\Psi(x,z)$, which represent pressure (P) and vertically polarized shear (SV) waves, respectively. The potentials due to the distributed source f(x) can, in turn, be synthesized in terms of a scalar point force excitation at $(x',z')=(x',0)$ as follows,

$$\Phi(x,z) = \frac{-1}{4\pi\rho\omega^2} \int f(x') \frac{\partial g_p}{\partial z}\, dx' \quad ; \quad \Psi(x,z) = \frac{-1}{4\pi\rho\omega^2} \int f(x') \frac{\partial g_s}{\partial x}\, dx' \tag{2}$$

where $g_{p,s}$ satisfy the two-dimensional (x,z) wave equations

$$(\nabla^2 + k_{p,s}^2) g_{p,s}(x,z;x',z') = -4\pi\, \delta(x-x')\delta(z-z') \quad , \quad k_{p,s} = \omega / v_{p,s} \tag{3a}$$

subject to a radiation condition at $|\underset{\sim}{R}| \to \infty$, where $\underset{\sim}{R}=(x,z)$. In (3a), $v_{p,s}$ are the compressional and shear wave propagation speeds

$$v_p = \sqrt{(\lambda+2\mu)/\rho} \quad , \quad v_s = \sqrt{\mu/\rho} \tag{3b}$$

The solution of (3a) is given by

$$g_{p,s} = i\pi H_o^{(1)}(k_{p,s} r) \qquad r = \sqrt{(x-x')^2 + (z-z')^2} \tag{4}$$

where $H_o^{(1)}$ is the Hankel function. In terms of the potentials in (2), the displacements in the horizontal (x) and vertical (z) directions are given by

$$u(x,z) = \frac{\partial \Phi(x,z)}{\partial x} - \frac{\partial \Psi(x,z)}{\partial z} \quad ; \quad w(x,z) = \frac{\partial \Phi(x,z)}{\partial z} + \frac{\partial \Psi(x,z)}{\partial x} \tag{5a}$$

and the vertical normal stress component by

$$\sigma_{zz}(x,z) = \lambda \left[\frac{\partial^2 \Phi(x,z)}{\partial x^2} + \frac{\partial^2 \Phi(x,z)}{\partial z^2} \right] + 2\mu \left[\frac{\partial^2 \Phi(x,z)}{\partial z^2} + \frac{\partial^2 \Psi(x,z)}{\partial x \partial z} \right] \tag{5b}$$

The potentials can be decomposed into plane wave spectra by Fourier transforming along the x-coordinate

$$\hat{\Lambda}(k,z) = \int \Lambda(x,z) e^{-ikx} dx \quad , \quad \Lambda = \Phi \text{ or } \Psi \tag{6a}$$

with the inverse $$\Lambda(x,z) = \frac{1}{2\pi} \int \hat{\Lambda}(k,z) e^{ikx} dk \tag{6b}$$

The resulting spectral amplitudes, expressed in terms of the spectrum $\hat{f}(k)$ of the source distribution f(x), are

$$\hat{\Phi}(k,z) = \frac{\hat{f}(k)}{2\rho\omega^2} e^{i\kappa_p z} \quad , \quad \hat{\Psi}(k,z) = \frac{\hat{f}(k)k}{2\rho\omega^2\kappa_s} e^{i\kappa_s z} \quad , \quad \kappa_{p,s} = \sqrt{k_{p,s}^2 - k^2} \tag{7}$$

with $\text{Im}\, \kappa_{p,s} \geq 0$. By inserting (7) into (6b), one obtains the plane wave spatial

spectrum representations for Φ and Ψ, and by inserting into (5) and performing the partial differentiations on the integrands, one obtains the corresponding representations for the displacements and normal stresses.

This completes the formulation and formal solution of the problem.

GAUSSIAN BEAM EXPANSION

For reasons stated in the Introduction, we now express the solution for the potentials and displacements in the previous section in terms of a self-consistent discretized Gaussian beam expansion over a configuration-wavenumber phase space lattice [6] (see Fig. 1). For the aperture function f(x), this expansion becomes

$$f(x) = \sum_n \sum_m A_{mn} \overset{v}{w}(x - mL_x) e^{in\Omega x} \tag{8}$$

where $\overset{v}{w}(x)$ is a normalized Gaussian window function defined by

$$\overset{v}{w}(x) = (\sqrt{2}/L_x)^{1/2} \exp(-\pi x^2/L_x^2) \quad , \quad \int |\overset{v}{w}(x)|^2 dx = 1 \tag{9}$$

The spatial displacement index m locates each Gaussian envelope along the space coordinate x, whereas the spectral displacement index n (see (8)) tags the superimposed linear phase shift. The spatial lattice separation L_x (the width of the Gaussian) and the spectral separation Ω (the width of its spectrum; see (14)), respectively, are constrained by the condition

$$\Omega L_x = 2\pi \tag{10}$$

The amplitude coefficients are expressed in terms of a biorthogonal function $\gamma(x)$,

$$A_{mn} = \int f(x) \gamma^*(x - mL_x) \exp(-in\Omega x) dx \tag{11}$$

where $\gamma(x)$ is determined from the biorthogonality relation

$$\int \overset{v}{w}(x) \gamma^*(x - mL_x) \exp(-in\Omega x) dx = \delta_m \delta_n \quad , \quad \delta_q = \begin{cases} 1 & \text{for } q=0 \\ 0 & \text{for } q \neq 0 \end{cases} \tag{11a}$$

and the asterisk denotes the complex conjugate. For the Gaussian window in (9), the function $\gamma(x)$ is given by [6]

$$\gamma(x) = \left(\frac{1}{\sqrt{2}L_x}\right)^2 \left(\frac{K_o}{\pi}\right)^{-3/2} \exp\left(\pi \frac{x^2}{L_x^2}\right) S_j \quad , \quad S_j = \sum_{j > (x/L_x) - 1/2}^{\infty} (-1)^j \exp\left(-\pi \left(j + \frac{1}{2}\right)^2\right) \tag{12}$$

with $K_o = 1.85407468$ representing the complete elliptic integral of the first kind of argument 1/2.

A similar expansion can be performed in the spectral domain. Here,

$$\hat{f}(k) = \sum_n \sum_m A_{mn} \hat{w}(k - n\Omega) \, e^{-imkL_x} \tag{13}$$

where

$$\hat{w}(k) = \left(\sqrt{2} L_x\right)^{1/2} \exp\left(-\pi \frac{k^2}{\Omega^2}\right) \tag{14}$$

is the spatial Fourier spectrum of $\overset{v}{w}(x)$. The evident symmetry of the spatial and spectral forms of the expansion facilitates simultaneous interpretation of

wave phenomena in the spatial and spectral domains. The index n in (13) places the spectral peaks at $k_n = n\Omega$, thereby identifying

$$\theta_{p,s}^{(n)} = \sin^{-1}(2\pi n/k_{p,s}L_x) \tag{14a}$$

later on, as the angle of tilt of the P and S beam axes away from the normal to the aperture.

The Gaussian beam expansions for the potential and displacement fields in, and away from, the aperture plane can be obtained by substituting (8) into (2), and (5) (spatial superposition form), or by substituting (13) into (6b) and (7), and (5) (plane wave spectral form). Choosing the latter, we find

$$\left\{\Phi(x,z),\ \Psi(x,z)\right\} = \frac{(\sqrt{2}L_x)^{1/2}}{4\pi\rho\omega^2}\sum\sum A_{mn}\left\{B_{1mn}(x,z),\ B_{2mn}(x,z)\right\} \tag{15}$$

and

$$u = \frac{(\sqrt{2}L_x)^{1/2}}{4\pi\rho\omega^2}\sum\sum A_{mn}\left\{\frac{\partial B_{1mn}(x,z)}{\partial x} - \frac{\partial B_{2mn}(x,z)}{\partial z}\right\} \tag{16a}$$

$$w = \frac{(\sqrt{2}L_x)^{1/2}}{4\pi\rho\omega^2}\sum\sum A_{mn}\left\{\frac{\partial B_{1mn}(x,z)}{\partial z} + \frac{\partial B_{2mn}(x,z)}{\partial x}\right\} \tag{16b}$$

where the beam functions $B_{1,2mn}$ are defined by the integrals

$$B_{1mn}(x,z) = \int_{-\infty}^{\infty} \exp(i\hat{f}_p(k))dk \ ; \ B_{2mn}(x,z) = \int_{-\infty}^{\infty} \frac{k}{\kappa_s}\exp(i\hat{f}_s(k))dk \tag{17}$$

with

$$\hat{f}_{p,s}(k) = k(x - mL_x) + \kappa_{p,s}z + \frac{1}{4\pi}(kL_x - 2\pi n)^2 \tag{18}$$

These expansions, which are valid anywhere in the half space $z>0$, reduce to their aperture plane form when $z \to 0^+$. The beam integrals become physically more transparent when they are expressed in the angular spectrum form in the local rotated beam-centered (ξ,η) coordinates (see Fig. 1).

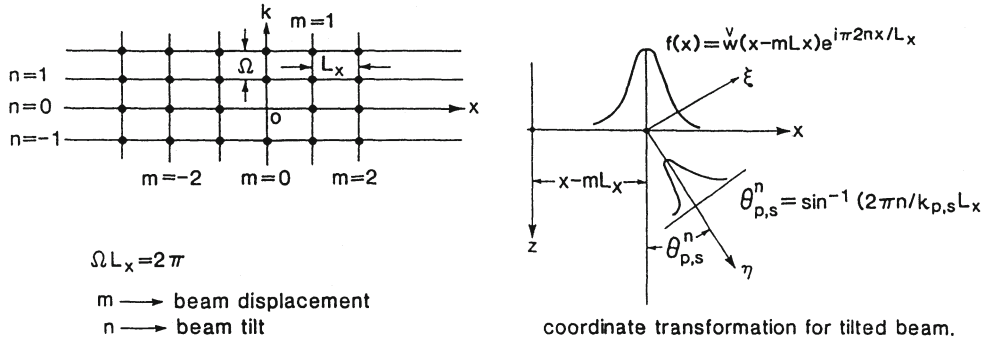

Fig. 1 Body force distribution in an infinite domain.

APPROXIMATE EVALUATION OF THE BEAM INTEGRALS

Saddle Point Asymptotics

Because the phase defined in (18) varies rapidly at sufficiently large distances away from the aperture plane, the beam integrals there can be evaluated asymptotically by the saddle point method, following in the complex k-plane the paths of steepest descent through the saddle points $k_{p,s}^{(o)}$ at which the functions are stationary. This yields [7]

$$\begin{Bmatrix} B_{1mn}(x,z) \\ B_{2mn}(x,z) \end{Bmatrix} = \begin{Bmatrix} 1 \\ k_s^{(o)}/\kappa_s^{(o)} \end{Bmatrix} \left(\frac{-2\pi}{id^2\hat{f}_{p,s}(k_{p,s}^{(o)})/dk_{p,s}^{(o)2}} \right)^{1/2} \exp\left(i\hat{f}_p(k_{p,s}^{(o)})\right) \quad (19)$$

with the saddle points $k_{p,s}^{(o)}$ defined by

$$d(\hat{f}_{p,s}(k_{p,s}^{(o)})/dk_{p,s}^{(o)}) = 0 \quad (20)$$

Complex Source Point Model

The complex source point (CSP) method furnishes a useful alternative to approximating the beam integrals in the paraxial region. As is well known [8,9], assigning complex values $\bar{\xi}'=0$, $\bar{\eta}'=ib_{p,s}$ to the source coordinates in the two dimensional free space potential Green's function in (4) generates a beam-like wavefield that continues to satisfy the source free wave equation and outgoing wave condition. At moderate distances, the analytically continued solution reduces to

$$g_{p,s} \sim i\pi \left(\frac{2}{\pi k_{p,s}\bar{r}} \right)^{1/2} \exp(ik_{p,s}\bar{r} - i\pi/4) \; ; \; \bar{r}=\sqrt{\xi^2+(\eta-ib_{p,s})^2} \; , \; Re(\bar{r})>0 \quad (21)$$

where $\bar{r}$ is the complex distance to the observer.

In the CSP formulation, the potential fields in (15) can be written as

$$\begin{Bmatrix} \Phi(x,z) \\ \Psi(x,z) \end{Bmatrix} = k_{p,s} \frac{(\sqrt{2}L_x)^{1/2}}{4\pi\rho\omega^2} \sum A_{mn} e^{-k_{p,s}b_{p,s}} \begin{Bmatrix} \partial g_p/\partial z \\ \partial g_s/\partial x \end{Bmatrix} \quad (22)$$

and the displacements in (16) as

$$\begin{Bmatrix} u \\ w \end{Bmatrix} = \frac{(\sqrt{2}L_x)^{1/2}}{4\pi\rho\omega^2} \sum A_{mn} \left[k_p e^{-k_p b_p} \begin{Bmatrix} \partial^2/\partial x\partial z \\ \partial^2/\partial z^2 \end{Bmatrix} g_p - k_s e^{-k_s b_s} \begin{Bmatrix} \partial^2/\partial x\partial z \\ -\partial^2/\partial x^2 \end{Bmatrix} g_s \right] \quad (23)$$

The expressions in (21), (22) and (23) have been used in the numerical calculations that follow.

NUMERICAL RESULTS

A sequence of numerical calculations has been carried out in order to: (1) assess the validity of the asymptotic complex source point (CSP) formulation to represent the asymptotic beam integrals, and (2) gain insight into how the choice of parameters in the Gaussian beam lattice representation of the aperture excitation affects the behavior of the elastic wave fields. Data have been generated for a range of beam basis elements spanning the interval from very wide to very narrow in the aperture plane. Both near and far fields of the potentials and displacements have been determined from (15) and (16) by asymptotic evaluation of the beam integrals of (17) for test aperture fields having a linear phase taper with (a) a tapered (cosine^2),and (b) a uniform amplitude profile. Due to space limitations, representative numerical plots cannot be included here but the outcome of the calculations is described in the text.

Beam Integral Asymptotics vs. CSP

Results from asymptotic approximation of the beam integrals (BI) and their CSP representation have been compared with a reference solution obtained by direct numerical integration of (2) and (5). Figure 2 shows a typical comparison (selected from a comprehensive set of data) between beam integrals evaluated asymptotically from (19) and by CSP from (21). For the narrow non-tilted beam ($L_x=0.2\lambda_p$), with observations at $R=5\lambda_p$, CSP is seen to reproduce the BI results within the angular regions $|\theta_p|\leq 80°$, $|\theta_s|\leq 42°$; agreement for the displacements in this region is to within 1%. Narrow tilted beams ($|n|>0$) have evanescent spectra away from the aperture plane ($\theta_{p,s}^{(n)}=\sin^{-1}(2n\pi/k_{p,s}L_x)$ is complex), and they therefore contribute negligibly in their far zones, which have already been reached at $R=5\lambda_p$. On the other hand, wide tilted beams ($|n|>0$) generated by wide basis elements in the aperture plane would be important contributors in the far zone. In general, for a given index n, $\Phi-$beams are tilted more than $\Psi-$beams. However, with increasing tilt, the wide beams become more asymmetric, and the BI results are therefore less accurately represented by CSP asymptotics. It has been found that CSP synthesis with non-tilted narrow-waisted beams works well in the intermediate and far zones, whereas the contrary is true when synthesizing with wide beams.

Smoothly Tapered Aperture Profile

Narrow beam synthesis. For narrow beams with respect to aperture width, the A_{mn} expansion coefficients in (8) for a smoothly tapered aperture field profile are known to be concentrated around the $n=0$ line, and the A_{mo} coefficients can be determined directly by sampling the profile, thereby avoiding need for evaluating the integral in (11) [10]. For aperture plane synthesis, the individual $n=0$ basis fields sample narrow regions, but the resulting spectral gaps can be filled by small but essential contributions from the $|n|>0$ elements. Away from the aperture plane, the (tilted) beams corresponding to $|n|>0$ are evanescent and therefore negligible except in the very near zone. For the parameters in Fig. 2, the $|n|>0$ beams can already be omitted at $R=5\lambda_p$, which is in the "far zone" of each element. CSP synthesis with nontilted beams is seen to be adequate, and the number of beams required is relatively small (27 beams: $|m|\leq 13$, $|n|=0$) (Fig. 3). Results obtained for phased aperture distributions (not shown) indicate that use of the same number of beams yields comparable accuracy in the far field.

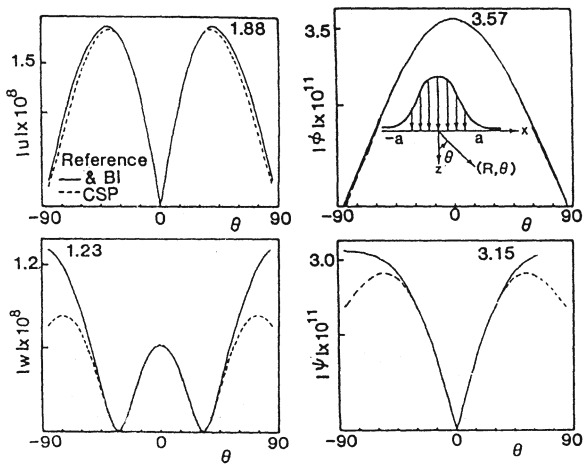

Fig. 2

Response at $R=5\lambda_p$ to a body force distribution defined by a single Gaussian basis function $f(x)=(\frac{\sqrt{2}}{L_x})^{1/2}e^{-\pi(x^2/L_x^2)}$

Narrow non-tilted beams: $L_x=0.2\lambda_p$, $n=0$. Beam parameters (Fresnel lengths): $b_p=0.04\lambda_p$, $b_s=0.07\lambda_p$.

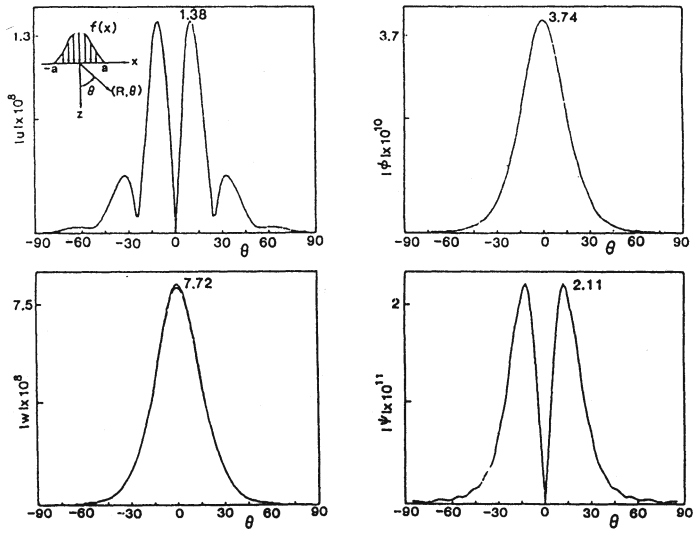

Fig. 3

Radiation pattern at $R=5\lambda_p$ using 27 ($|m|\leq 13, n=0$) narrow beam ($L_x=0.2\lambda_p$) elements. Fresnel zone of aperture: $D_{ap}=(2a)^2/\lambda_p=25\lambda_p$. Aperture profile: $f(x)=\cos^2(\pi x/2a)$. Aperture width: $2a=5\lambda_p$. Ref., BI and CSP coincide.

Wide beam synthesis. For wide basis elements with L_x extending over several aperture widths (results not shown), phasings $|n|>0$ are important but shifted locations $|m|>0$ are much less so. The expansion coefficients A_{on} now have amplitudes that match the far zone angular pattern at the spectral sampling points [10]; this allows the estimation of these coefficients without going through the numerical evaluation of (11).

Matched beams. Basis elements matched to the aperture size ($L_x\approx 2a$) afford still another synthesis option. Now, the contributing elements (m,n), with approximately equal weighting, are localized around the central element $m=n=0$, which gives the dominant contribution for a smooth nonphased aperture field profile. Therefore, synthesising quasi-Gaussian inputs is fairly efficient but accounting for strong deviations is not. One feature of interest with matched beams is the good fit of the $m=n=0$ beam contribution to the main lobe of Φ and w in the far field pattern.

Abruptly Truncated Aperture Profile

A much more severe test of the beam synthesis technique is posed by an abruptly truncated aperture profile. Results reveal that narrow basis elements now have amplitude coefficients that include more $|n|>0$ contributions, and the A_{mo} coefficients reveal irregularities and spikes caused by the discontinuities at the profile edges. Aperture synthesis with narrow beams does correspondingly more poorly but near and far zone synthesis proceeds as before, and with comparable accuracy.

CONCLUSIONS

A self-consistent superposition of Gaussian basis elements and the corresponding Gaussian beam propagators on a configuration-wavenumber phase space lattice has been utilized here for the rigorous representation of finite planar source distributions and the resulting radiated fields in an unbounded homogeneous elastic solid. From comprehensive results for two simple linearly phased aperture profiles with smoothly tapered and abruptly truncated amplitude behavior, only a sample of which has been included here, it has been learned how the choice of nontilted and tilted narrow, wide or matched beams with respect to the aperture size affects the field synthesis, how well asymptotic approximations of the beam propagator integrals (BI) agree with a numerical reference solution, and how well the asymptotic BI can be approximated by more convenient complex source point (CSP) fields. Narrow beam synthesis away from the aperture plane involves nontilted ($n = 0$) beams only (the tilted $|n| > 0$ beams are evanescent), and these beams can be tracked along almost real trajectories because of the small complex displacement component of the narrow beam source location. This ray-like behavior makes narrow beams interesting candidates for negotiating complicated environments at high frequencies.

The algorithm developed so far is for two-dimensional fields but extension to three dimensions is in progress. It is intended to use this technique for accurate modeling of transducer outputs. The Gaussian beam algorithm may also furnish a useful NDE option for describing scattering due to induced source distributions in fault zones. These matters remain to be explored.

ACKNOWLEDGEMENT

This work has been supported by the Air Force Office of Scientific Research under Grant No. AFOSR-86-0318.

REFERENCES

1. V. Cerveny, M.M. Popov and I. Psencik, Geophys. J.R. astr. Soc., 70, 109, (1982).
2. B.P. Newberry, T.A. Gray, E.F. Lopes and R.B. Thompson, in Review of Progress in Quantitative NDE, D.O. Thompson and D.E. Chimenti, Eds., (Plenum Press, NY, 1986), Vol. 5A, pp. 127-138.
3. J.J. Wen and M.A. Breazeale, J. Acoust. Soc. Am., 83, 1752 (1988).
4. J.J. Maciel and L.B. Felsen, "Systematic Study of Fields Due to Extended Apertures by Gaussian Beam Discretization," to be published in IEEE Trans. Antennas Propag.
5. J.D. Achenbach, Wave Propagation in Elastic Solids, North Holland (1973).
6. M.J. Bastiaans, Proc. IEEE, 68, 538 (1980).
7. L.B. Felsen and N. Marcuvitz, Radiation and Scattering of Waves, (Prentice-Hall, NJ, 1973).
8. L.B. Felsen, Philips Res. Repts., 30, 187 (1975).
9. L.B. Felsen, in Symposia Matematica, Istituto de Alta Matematica, (Academic Press, NY, 1976) pp. 39-56.
10. P.D. Einziger, S. Raz and M. Shapira, J. Opt. Soc. Am., 3, 508 (1986).